Atomic structures and bondings of β- and spinel-$Si_{6-z}Al_zO_zN_{8-z}$ by first-principles calculations

Kazuyoshi Tatsumi,* Isao Tanaka, Hirohiko Adachi, and Masato Yoshiya†
Department of Materials Science and Engineering, Kyoto University, Sakyo, Kyoto, 606-8501 Japan
(Received 30 April 2002; published 8 October 2002)

First-principles calculations of β- and spinel-sialons ($Si_{6-z}Al_zO_zN_{8-z}$) have been systematically made by a plane-wave pseudopotentials method, in order to find out atomic arrangements, bondings, and electronic structures of optimized structures. Al-O and Si-N bonds are found to be clearly preferred as compared with Si-O and Al-N bonds in two kinds of crystals. In the optimized structures, the band gap can be roughly approximated as the weighed average of those for end members, i.e., Si_3N_4 and Al_3O_3N. Few impuritylike states are formed near the band edges. Averaged bond-lengths of Al-X and Si-X (X=N and O) are almost constant and independent of z for a given site of each crystal. All of these results are consistent to experimental information thus far been available by nuclear magnetic resonance and extended x-ray absorption fine structures. Calculations of formation energies of β-sialons using supercells composed of 56 atoms suggest ordering of solute atoms to form a unique local structure is not likely to take place.

DOI: 10.1103/PhysRevB.66.165210 PACS number(s): 71.20.Nr, 71.20.Gj, 61.66.Dk

I. INTRODUCTION

Silicon nitride has been widely studied as high-temperature structural components and gate dielectrics in microelectronics applications. The recent discovery of the cubic spinel phase[1] as the third polymorph opened a door toward application of this compound for a new wide-gap semiconductor, since it is theoretically predicted to exhibit a direct bandgap.[2] Candidates for active dopants for *n*-and *p*-type conductors have also been predicted by first-principles calculations.[3]

Wide solubility range of Al and O in hexagonal Si_3N_4 with α and β forms was reported by two groups independently.[4,5] The solid solution has been called sialon whose chemical formula is often denoted by $Si_{6-z}Al_zO_zN_{8-z}$. The solubility limit in the β phase is known to be approximately $z=4$ at around 1700 °C. Recently sialons have also been reported in the spinel phase.[6]

Experimental investigation to elucidate atomic structure of β-sialons has been made by three kinds of techniques, namely, neutron diffraction, magic angle-spinning nuclear magnetic resonance (MAS-NMR), and extended x-ray absorption fine structures (EXAFS). Rietveld refinement of the neutron diffraction profile of β-sialons concluded that oxygen atoms slightly preferred to occupy the $2c$ site of N according to Wyckoff's notation.[7,8] ^{27}Al and ^{29}Si MAS-NMR of β-sialons have been measured systematically.[9–12] They have concluded that the local environments of both Al and Si atoms in β-sialon were far from random distribution. According to their interpretation, formation of Si-N and Al-O bonds was preferred as compared to Si-O and Al-N bonds. NMR of spinel-sialon was recently reported by Sekine *et al.*[6] EXAFS at Al-K and Si-K edges of β-sialons[13] is also suggestive of the preference of Si-N and Al-O bondings. It was concluded that the bond lengths of Si-N/O and Al-O/N do not depend so much on the solute concentration. The distribution of the bond length is found to be rather narrow.

First-principles calculations of β-sialons were pioneered by Tanaka *et al.* using model clusters.[14] They also measured Young's modulus and Raman peak shifts. The lattice softening due to the presence of solutes was then ascribed to the weakening of the covalent bond strength. First principles band structure calculations were made by Ching, Huang, and Mo[15] about a decade later. They calculated bulk modulus of β-sialons of different solute concentrations, and experimental trend for the solution softening was successfully reproduced. They pointed out that the substitution resulted in the formation of impurity-like states in the upper portion of the band-gap. This brought about the significant decrease in the band-gap from 4.2 eV ($z=0$) to 1.3 eV ($z=4$). Although local density approximation (LDA) used in their work may underestimate the band gap in general, the band-gap smaller than the critical value for visible transparency (around 3.2 eV) should be inconsistent to the reality, because β-sialon materials look transparent and colorless when fabricated without additives in the present author's experience.[16,17] Okatov and Ivanovskii. investigated the atomic arrangements of β-sialons using the tight-binding band structure method based on extended Hückel approximation.[18] From the calculated total energies and bond analysis with overlap populations, they claimed the formation of ''quasi-one-dimensional impurity channel'' in β-sialons in which Al and O atoms were ordered. However, they did not referred to the effect of the lattice relaxation induced by the solute atoms. Band gaps of β-sialons were not discussed, either. In the present study, we aim at detailed study on the relationship between atomic arrangements and energetics of sialons employing first-principles calculations. Bond preferences in both β- and spinel-sialons are investigated systematically. Electronic states of the optimized structures are investigated as well. Then possible clustering of solute atoms in β-sialons is discussed.

II. COMPUTATIONAL PROCEDURE

Present calculations were performed using the first-principles plane wave-basis pseudopotential method[19] within

the density functional theory. Exchange-correlation effects were taken into account by the generalized gradient approximation.[20] Ultrasoft pseudopotentials of Vanderbilt's type[21] were adapted for all the atomic species. They were constructed with two projector functions in each *sp* channels of all the elements. The plane-wave cutoff energy E_{cut} was set to be 380 eV throughout this study. The **k**-points used for numerical integration were chosen at the mesh points by Monkhorst-Pack's scheme.[22]

We examined energetics of β- and spinel-sialons systematically using primitive cells of β- and spinel-Si_3N_4. Both of them contain 14 atoms. We will call these models primitive cell models. Calculations were made for seven different solute concentrations as denoted by z in $Si_{6-z}Al_zO_zN_{8-z}$, i.e., $z=0$, 1, 2,..., 6. The mesh points in the **k**-space correspond to 27 and 32 **k**-points in the whole Brillouin zone, for β- and spinel-sialons, respectively. The convergence of the relative total energy difference between the different atomic arrangements of sialons at the same composition was examined up to the cutoff energy of 800 eV and the number of **k**-points of 72 and 108 for β- and spinel-sialons. It was confirmed to be better than 1 meV/atom with the present computational conditions. Additional calculations using supercells of β-Si_3N_4 were made in order to seek for more preferable atomic arrangements with less restricted structures.

Structural relaxation induced by the substitutions was taken into account for all the calculations. Initial structures were obtained by simple substitutions of Al/O atoms to Si/N sites. By imposing only the space group of the initial structures, optimization of all lattice parameters was made. The optimization was truncated when the maximum residual force on atoms became smaller than 0.05 eV/Å.

Entropy effects were not taken into account in the present calculations, although both configurational and vibrational entropies should have non-negligible contributions at high temperatures where sialons are normally synthesized. Strictly speaking the bond and site preference of sialons obtained in the present study corresponds only to those at the ground state. However, as will be seen later in this paper, the information well explains many experimental results thus far been available.

III. RESULTS AND DISCUSSION

A. Formation energy of sialons

Energetics of β- and spinel-sialons have been examined systematically using the primitive cell model. They have a formula of $Si_{6-z}Al_zO_zN_{8-z}$ ranging from $z=0$ to 6. In order to perform systematic investigations, we included the compositions of $z=5$ and 6 that correspond to a supersaturated sialon and a hypothetical ''alon,'' respectively. A large number of atomic arrangements with different solute configurations can be obtained by simple substitution of Al and O atoms to Si and N sites of β-Si_3N_4 even within the primitive cell model. It is too large to examine all of the nonequivalent initial structures. However, many of the initial structures hold the same number of nearest-neighbor bonds, i.e., Al-O, Si-N, Al-N, and Si-O bonds, in the unit cell. In other words, they have the same ''bond configurations.'' For β-$Si_{6-z}Al_zO_zN_{8-z}$, supposing all cations are fourfold-coordinated and all anions are threefold-coordinated as in the original β-Si_3N_4 crystal, the bond configuration can be unambiguously determined by the number of the Al-O and Si-N bonds in the unit cell. The number of X-Y bonds per the formula of $Si_{6-z}Al_zO_zN_{8-z}$ will be denoted by $N_{\text{X-Y}}$. In β-sialons, a simple algebra can find following set of equations:

$$N_{\text{Al-N}}=4z-N_{\text{Al-O}},$$

$$N_{\text{Si-N}}=24-7z+N_{\text{Al-O}},$$

$$N_{\text{Si-O}}=3z-N_{\text{Al-O}}. \tag{1}$$

This means that all $N_{\text{X-Y}}$ can be uniquely determined for given z and $N_{\text{Al-O}}$.

For spinel-$Si_{6-z}Al_zO_zN_{8-z}$, four sixfold-coordinated sites (O sites) and two fourfold-coordinated sites (T sites) coexist as cationic sites in the primitive cell. The fraction of the Al atoms at the T sites f_{T} additionally affects the bond configurations. In spinel-sialons, the following set of equations can be found:

$$N_{\text{Al-N}}=6z-2zf_{\mathrm{T}}-N_{\text{Al-O}},$$

$$N_{\text{Si-N}}=32-10z+2zf_{\mathrm{T}}+N_{\text{Al-O}},$$

$$N_{\text{Si-O}}=4z-N_{\text{Al-O}}. \tag{2}$$

We have selected arbitrary one representative from the atomic arrangements that hold the same bond configuration in the unit cell. The total energy of the representative model was investigated as a function of the bond configuration. Figure 1 shows the results. Here the bond configurations are described by $N_{\text{Al-O}}$. The energy in Fig. 1 is the formation energy of sialons E^F per a pair of Al+O:

$$E^F=\frac{1}{z}\left[E_t(\mathrm{Si}_{6-z}\mathrm{Al}_z\mathrm{O}_z\mathrm{N}_{8-z})-\left(\frac{z}{3}[E_t(\mathrm{Al}_2\mathrm{O}_3)+E_t(\mathrm{AlN})]+\frac{6-z}{3}E_t(\mathrm{Si}_3\mathrm{N}_4)\right)\right]. \tag{3}$$

$E_t(Si_{6-z}Al_zO_zN_{8-z})$ is the total energy of sialons per formula. The reference states for the formation energy are chosen to be corundum-Al_2O_3, wurtzite-AlN, and β-Si_3N_4 for β-$Si_{6-z}Al_zO_zN_{8-z}$. For spinel-$Si_{6-z}Al_zO_zN_{8-z}$, corundum-Al_2O_3, rocksalt-AlN, and spinel-Si_3N_4 have been chosen. $E_t(Al_2O_3)$, $E_t(AlN)$, and $E_t(Si_3N_4)$ are total energies per formula of these references. The rocksalt structure of AlN has been chosen in the latter case, since it is known to be more stable under high pressures of approximately 10 GPa. The difference in $E_t(AlN)$ between the two structures by the present calculation was 0.42 eV under the equilibrium condition. In the Si-Al-O-N system, some intermediate phases have been reported between β-Si_3N_4 and our reference phases. However, the crystallographic information on them is too limited to be used as reliable references. We

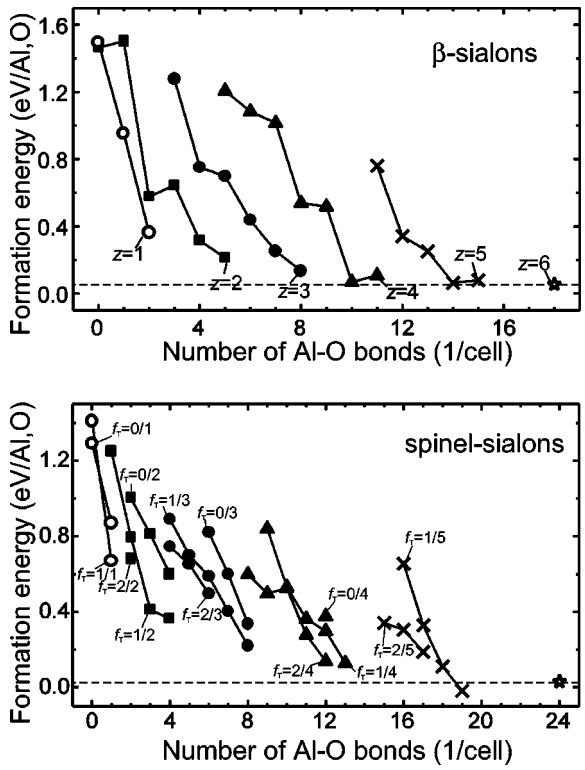

FIG. 1. Dependence of the formation energy given by Eq. (3) on the bond-configuration within the primitive cell models: (Top) for β-sialons, (bottom) for spinel-sialons. Denominators of f_T indicate corresponding composition parameter z.

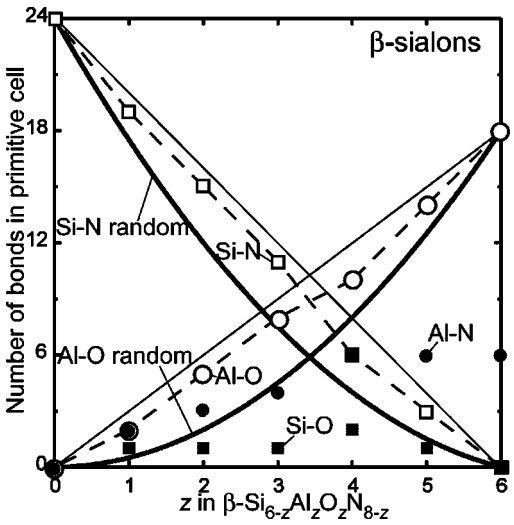

FIG. 2. Numbers of Al-O (open circles), Si-N (open squares), Al-N (closed circles), and Si-O (closed squares) bonds in the lowest energy models of β-sialons. Two referential cases are shown together. They are the numbers of bonds in the random models in which no bonds are preferred (thick solid curve) and those in the models at the segregation limit in which Si_3N_4 and Al_3O_3N phases are separately present (thin solid line).

therefore ignored any of these phases on the evaluation of E^F. As a result, there may be a small ambiguity in the absolute values of E^F in Fig. 1. But it does not affect the relative comparison of the formation energies at all.

A clear trend can be found in Fig. 1. E^F decreases with the increase of $N_{\text{Al-O}}$ for both β- and spinel-sialons. The solute atoms, Al and O prefer to be bound with each other. The energy gain associated with the pairing of Al-O is the order of a few tenth of eV per a pair of Al and O. Reduction of the number of Al-O pairs is therefore prohibitively expensive at any compositions. As for spinel-sialons, dependence of the total energy on f_T, i.e., the fraction of Al atoms at the T sites, is much smaller than that on $N_{\text{Al-O}}$. When compared at the same $N_{\text{Al-O}}$, larger f_T resulted in smaller total energy in most of cases. However, the maximum $N_{\text{Al-O}}$ for a given z that provides lowest energy is obtained for an intermediate value of f_T. Therefore, there is a clear priority to increase $N_{\text{Al-O}}$ than f_T for the spinel-sialons.

B. Bond preferences in sialons

The numbers of bonds of the lowest energy models are summarized in Figs. 2 and 3 as a function of z. The dependence of f_T for spinel sialons is shown together. Two model cases can be used to calculate $N_{\text{X-Y}}$. One is the model at the segregation limit in which Si_3N_4 and Al_3O_3N phases are separately present. Assuming that both Si_3N_4 and Al_3O_3N crystals are infinitively large, we can neglect the interface between two crystals. Then $N_{\text{Si-O}}$ is zero, and all other numbers of bonds are simply proportional to the composition as represented by z. The hypothetical values are shown by thin solid lines in the figure. The other is a random model in which no bonds are preferred. In the random model, we fixed the crystal structure. No exchange between cations and anions was allowed. The number of bonds in the random model can be obtained as follows.

For β-sialons,

$$N_{\text{Al-O}} = 1/2z^2,$$
$$N_{\text{Al-N}} = -1/2z^2 + 4z,$$
$$N_{\text{Si-N}} = 1/2z^2 - 7z + 24,$$
$$N_{\text{Si-O}} = -1/2z^2 + 3z. \tag{4a}$$

For spinel-sialons,

$$N_{\text{Al-O}} = 2/3z^2,$$
$$N_{\text{Al-N}} = -2/3z^2 + 16/3z,$$
$$N_{\text{Si-N}} = 2/3z^2 - 28/3z + 32,$$
$$N_{\text{Si-O}} = -2/3z^2 + 4z. \tag{4b}$$

They are shown in the figure as solid parabolic curves. Actual results obtained by the present calculations using primitive cells are plotted and connected by broken lines. In β-sialons, the results are close to those at the segregation limit. As long as we use the primitive cell model, we cannot reach the hypothetical segregation limit. However, the formation energy at the segregation limit can be evaluated by a separate calculation, which is shown in Fig. 1 using a broken

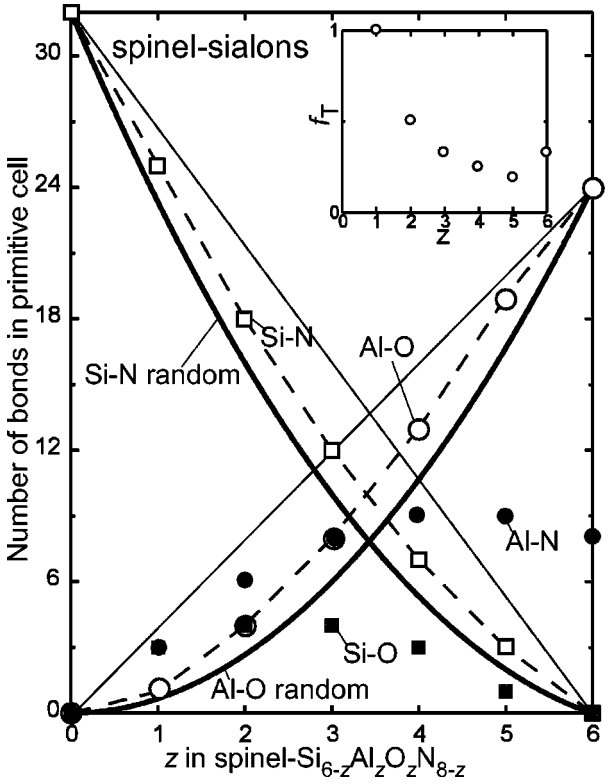

FIG. 3. Numbers of Al-O, Si-N, Al-N, and Si-O bonds in the lowest energy models of spinel-sialons at each composition. Two referential cases similar to those for β-sialons are shown together. Both of them are denoted in the same way as in Fig. 2. The inset shows the fraction of the Al atoms at the T sites, f_T, of the lowest energy models.

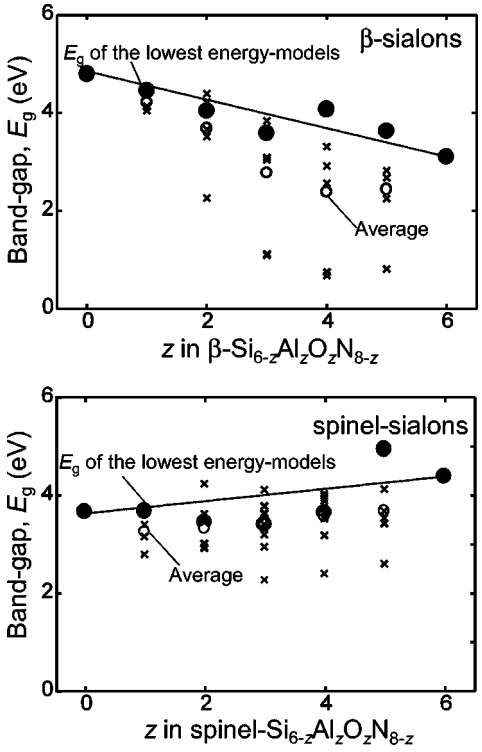

FIG. 4. (Top) Calculated band-gaps of β-sialons by the primitive cell models and (bottom) spinel-sialons. The band-gaps of the lowest energy models at each composition E_g are denoted by closed circles. Average values within all models at each composition are showed by open circles.

line. The formation energies of the lowest energy models are close to those at the segregation limit when $z \geqslant 4$. For $z<4$, the lowest energies obtained by the primitive cell models are greater than the energy at the segregation limit. This suggests that larger supercells than the primitive cell models may be used to reduce the total energy when $z<4$. Calculations using larger supercells will be described later in this paper. Combining information in Figs. 1 and 2, we can find that both $N_{\text{Si-N}}$ and $N_{\text{Al-O}}$ are maximized and $N_{\text{Si-O}}$ and $N_{\text{Al-N}}$ are minimized within the primitive cell model in order to reduce the energy. Si-N and Al-O bonds are clearly preferred as compared with Si-O and Al-N bonds.

For spinel sialons, f_T of the lowest energy models at $z \leqslant 5$ decreases monotonically with the increase of z as shown in Fig. 3. It is unity when $z=1$, which means that the first Al in the primitive cell of the spinel sialon prefers to occupy the tetrahedral site. The second to fifth Al in the primitive cell then prefers to occupy an octahedral site. Both of models at the segregation limit and random distributions were made with $f_T=\frac{1}{3}$ which corresponds to the random occupancy of tetrahedral/octahedral sites by Al atoms. Similar to the case of Fig. 1, both $N_{\text{Si-N}}$ and $N_{\text{Al-O}}$ are maximized and $N_{\text{Si-O}}$ and $N_{\text{Al-N}}$ are minimized in the lowest energy models. However, the deviation from the random model is smaller than that of β-sialons. The difference in the magnitude of deviation in the two crystals can be ascribed to the difference in the structure of primitive cells. We can expect to see a smaller deviation in spinel sialons using larger cells. However, it may not change our conclusion qualitatively Si-N and Al-O bonds are preferred as compared with Si-O and Al-N bonds.

C. Band-gap and electronic structures

In order to examine the difference in electronic structures of sialons with relation to the bond preferences, one-electron band-gap by the primitive cell models is plotted in Fig. 4. The band-gap E_g exhibits a wide variety among bond-configurations at the same composition. In the figure, the band-gap of the models showing the lowest total energy (E_g of the lowest energy model) is distinguished from the other E_g. This will be denoted by E_g^0. In β-sialons, E_g^0 is located close to the line that connects E_g of the end members, i.e., $E_g=4.9$ eV for $z=0$ and 3.6 eV for $z=6$. It is interesting that E_g^0 shows almost the highest value among the scattering of E_g. Figure 5 shows the density of states (DOS) of β-Si_3N_4 and two models for $z=2$ showing $E_g=2.3$ eV and $E_g=E_g^0=4.1$ eV. In the DOS of the model with the smaller E_g, a tail can be clearly seen near the bottom of the conduction band, and a few states are observed near the top of the valence band. The character of these states can be interpreted from local projected DOS (LPDOS) of the model showing $E_g=2.3$ eV. Figure 6 shows LPDOS of the model showing $E_g=2.3$ eV, together with the total DOS of the model. LPDOS for the orbitals of the following constituent atoms are

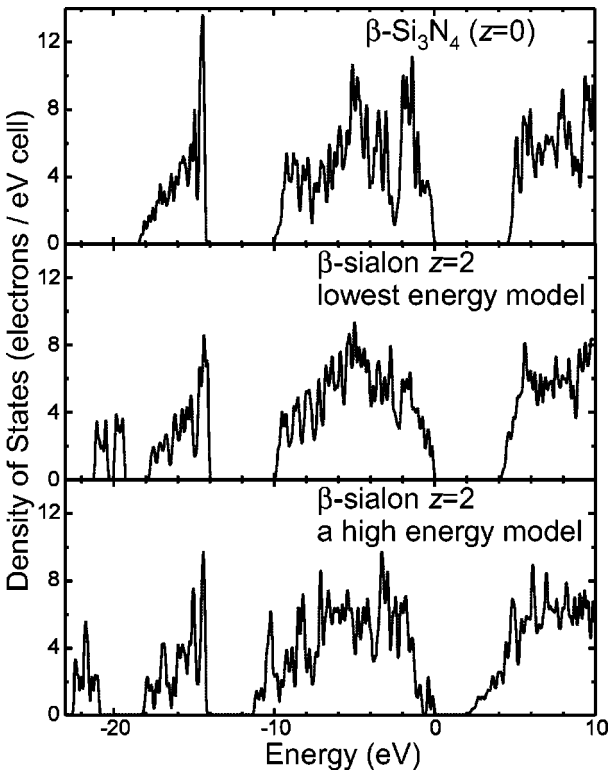

FIG. 5. (Top) Total density of states (DOS) of β-Si_3N_4, (middle) the lowest energy model of β-sialons at $z=2$ and (bottom) a high-energy model of β-sialons at $z=2$.

shown; Si coordinated by both O and N (2O, 2N), Si coordinated only by N (4N), N coordinated by both Al and Si (2Al, 1Si), and N coordinated only by Si (3Si). From these LPDOS's, it is clearly found that the tail near the conduction band edge are mainly composed of orbitals of Si coordinated by O. On the other hand, the states near the valence band edge are composed of orbitals of N coordinated by Al. In the energetically favorable model with $N_{\text{Al-O}}=5$ and $N_{\text{Si-N}}=15$, such impuritylike states cannot be found. This should be ascribed to the poverty of both Si-O and Al-N bonds, i.e., $N_{\text{Si-O}}=1$ and $N_{\text{Al-N}}=3$. We can therefore conclude that the decrease of E_g by the formation of the impurity-like states and the increase in the total energy have the same origin: That is the formation of Si-O and Al-N bonds. The band gaps of β-sialons of the most preferable bond-configurations are greater than 3.6 eV at any z value. This is consistent to the experimental observation that all β-sialons sintered without additives show optical transparency. We can also point out that much smaller theoretical E_g than the present E_g^0 as reported by Ching, Huang, and Mo.[15] can be ascribed to the lack of the optimization of bond configuration. As a matter of fact, they have reported the presence of impurity-like states in their DOS and local DOS similar to the case of the high-energy model shown in Figs. 5 and 6.

D. Bond-lengths in β-sialons

Bond-lengths in the optimized structures are analyzed in this section. Figure 7 shows average bond-lengths for the

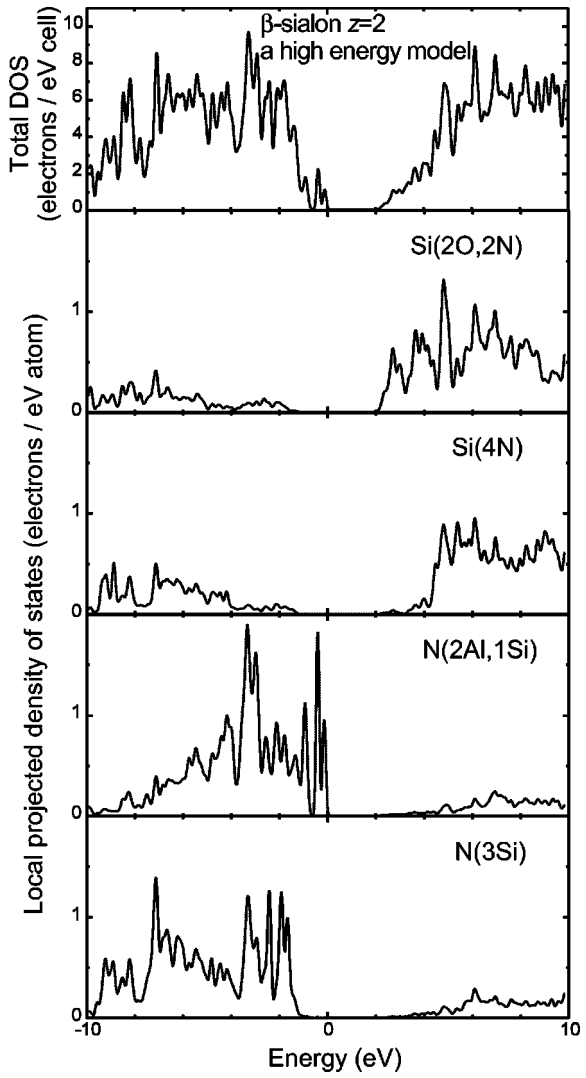

FIG. 6. Total DOS and local projected DOS near the band gap shown for the high-energy model of β-sialons at $z=2$. Local projected DOS of 4 atoms coordinated differently are shown. The coordinating atoms are indicated in the bracket.

β-sialons at $z=2$ with different $N_{\text{Al-O}}$. Clear trends can be seen for the bond-lengths of Al-O and Si-N, i.e., $d_{\text{Al-O}}$ and $d_{\text{Si-N}}$. The bond configurations containing fewer Al-O bonds are found to exhibit longer Al-O bonds. On the other hand, Si-N bonds became longer with the increase of the $N_{\text{Al-O}}$. The difference between $d_{\text{Al-O}}$ and $d_{\text{Si-N}}$ is 0.24 Å at $N_{\text{Al-O}}=1$. As the number of Al-O bonds increases, the difference became smaller. In the lowest energy model with $N_{\text{Al-O}}=5$, four bond lengths converged within the difference of 0.07 Å. It is very interesting that two kinds of bonds with Al, i.e., $d_{\text{Al-O}}$ and $d_{\text{Al-N}}$, have converged to almost the same value in the lowest energy model. Two kinds of Si-X bonds, i.e., $d_{\text{Si-O}}$ and $d_{\text{Si-N}}$, have converged as well. Figure 8 shows average bond lengths of lowest energy models for each z. The bond lengths are found to be almost constant and independent of z. $N_{\text{Al-O}}$ increases with the increase of z, which brings about the increase of the average bond length d_{all} as shown by a broken line in Fig. 8. d_{all} changes linearly from $d_{\text{Si-N}}$ at $z=0$ to

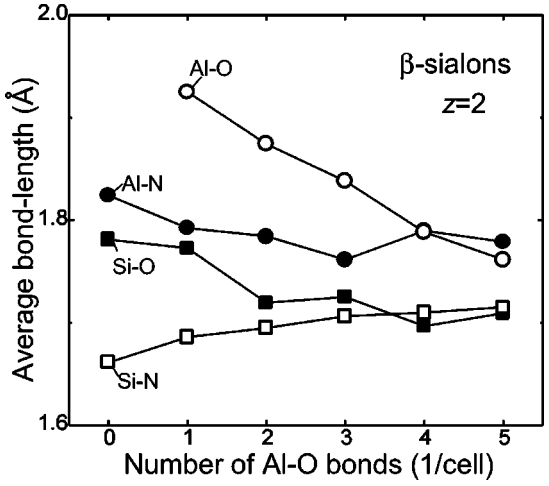

FIG. 7. Average bond-lengths of the primitive cell models for β-sialons at $z=2$; for Al-O (open circles), Al-N (closed circles), Si-N (open squares), and Si-O (closed squares).

$d_{\text{Al-O}}$ at $z=6$. This means that structural relaxation is minimal in the series of lowest energy models. The total energy of a low $N_{\text{Al-O}}$ model was much higher despite a significant structural relaxation. This implies that relaxation of bond lengths has little role in determining the preferable structure. We can conclude that the structure of β-sialons is determined in order to enrich $N_{\text{Al-O}}$ and $N_{\text{Si-N}}$ bonds with minimal distortion of the crystal structure.

Sjöberg *et al.* made EXAFS experiments of β-sialons with $z=1$ and 2.7 to compare the bond lengths of Si-O/N and Al-O/N.[13] They reported that both $d_{\text{Si-X}}$ and $d_{\text{Al-X}}$ are independent of the solute concentration, and their difference is approximately 0.1 Å. Our result on the lowest energy model shows very good agreement to the EXAFS results. If a higher energy model with a low $N_{\text{Al-O}}$ value is adopted, the difference in bond lengths should be much larger than the experimental results.

Experimental works of ^{29}Si and ^{27}Al MAS-NMR on β-sialons with $z=1$, 2, and 4 have revealed that Si can be only included in SiN_4 while Al can have a range of

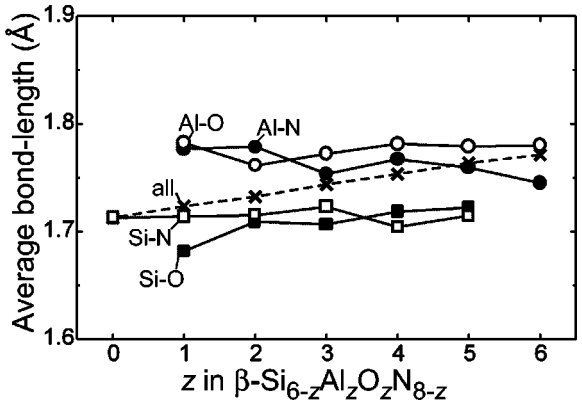

FIG. 8. Average bond-lengths of the lowest energy models of β-sialons at each composition; for Al-O (open circles), Al-N (closed circles), Si-N (open squares), Si-O (closed squares) bonds, and all bonds (crosses).

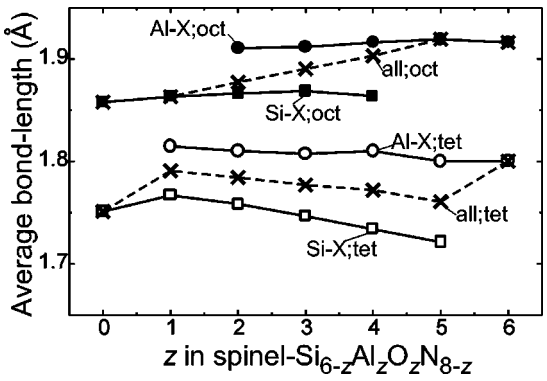

FIG. 9. Average bond lengths of the lowest energy models of spinel-sialons at each composition; for Al-X (X=N,O) of octahedral bonds (closed circles), Si-X of octahedral bonds (closed squares), Al-X of tetrahedral bonds (open circles), Si-X of tetrahedral bonds (open squares), and all octahedral and tetrahedral bonds (crosses).

AlO_xN_{4-x} $(0<x<4)$.[10] This indicates the absence of Si-O bonds, which shows good consistency with the present theoretical results.

E. Bond-lengths in spinel-sialons

Bond-lengths of spinel-sialons have been analyzed in the way similar to that for the β phase. At first sight the dependence of the bond-lengths on z is more complicated than that of the β phase. However, when cations at tetrahedral and octahedral sites are distinguished and average bond lengths of Al-X and Si-X bonds are used, a clear trend shows up. Figure 9 displays averaged bond lengths of lowest-energy models. For both Al-X and Si-X, the bond lengths with octahedral cations are greater than those with tetrahedral cations by approximately 0.1 Å. This is quite natural from the viewpoint of solid state chemistry in which the ionic radius of a cation at the tetrahedral site is usually taken to be smaller than that at the octahedral site. The average bond lengths $d_{\text{Si-X}}$ and $d_{\text{Al-X}}$, show little dependency on z, which is similar to the case of β-sialons. Differences in $d_{\text{Si-X}}$ and $d_{\text{Al-X}}$ are ranging from 0.04 to 0.05 and 0.05 to 0.08 Å for octahedral and tetrahedral sites, respectively. They are almost the same as the difference in β-sialons, i.e., is ranging from 0.04 to 0.07 Å.

d_{all} for bonds with octahedral cations increases linearly when the number of Al at the octahedral sites increases. Similar trend can be seen for d_{all} for bonds with tetrahedral cations from $z=0$ to 1 and $z=5$ to 6. However, d_{all} with tetrahedral cations decreases slightly with z in the range of $1\leqslant z\leqslant 5$. As learned from Fig. 3, the number of Al atoms at the tetrahedral sites, which is given by the product of z and f_{T}, is constant when $1\leqslant z\leqslant 5$. Only octahedral sites are occupied to increase z in this range. Since both of $d_{\text{Al-X}}$ and $d_{\text{Si-X}}$ do not change significantly with z, d_{all} with tetrahedral cations does not change remarkably when $1\leqslant z\leqslant 5$.

^{29}Si MAS-NMR results of spinel-sialon with $z=1.8$ and 2.8 were recently reported by Sekine *et al.*[6] They found two peaks that can be attributed to SiN_4 and SiN_6. No Si atoms

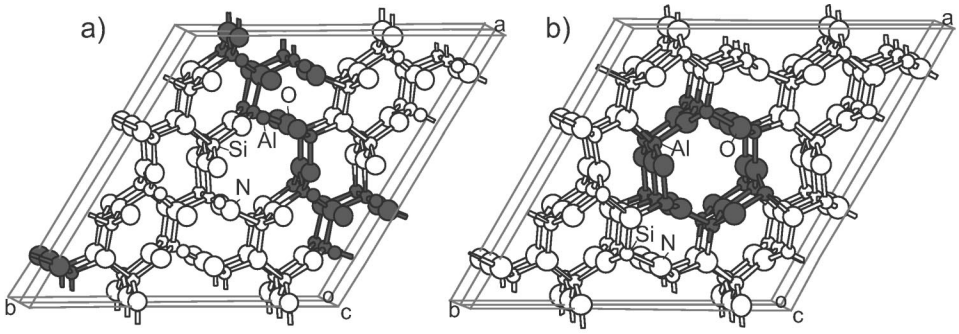

FIG. 10. Atomic arrangements of the two supercells of β-sialons. (Right) Solute Al and O atoms are arranged in a layer on the $(1\bar{1}00)$ plane. The composition is $z=2$, the number of Al-O bonds is 5.25 per $Si_{6-z}Al_zO_zN_{8-z}$. (Left) Solute Al and O atoms are arranged in a column along the c axis. The composition is $z=1.5$ and the number of Al-O bonds is 6 per $Si_{6-z}Al_zO_zN_{8-z}$ (the maximum value at this composition).

coordinated by any oxygen atoms were detected. This is consistent to our theoretical results, similar to the case of β-sialons.

F. Possibility of further clustering of solute atoms in β-sialons

When the primitive cell models were adopted, the lowest energy models at $1 \leqslant z \leqslant 3$ showed smaller $N_{\text{Al-O}}$ and $N_{\text{Si-N}}$ than those at the hypothetical segregation limit, and their total energies were notably higher than those for the segregation limit as discussed in Sec. III B. It is interesting whether the higher energy can be ascribed to the structural restriction by the use of the primitive cell models. If it is the case, the formation energies at $1 \leqslant z \leqslant 3$ can be reduced when larger supercells are used.

On the basis of the analysis of MAS-NMR spectra of β-sialons, Dupree *et al.* actually proposed a microdomain model in which Al+O-rich and Si+N-rich domains form layered structures.[10] Okatov and Ivanovskii very recently reported the extended Hückel tight binding calculations of β-sialons.[18] They claimed that ''quasi-one-dimensional impurity channel'' could be formed in β-sialons in order to reduce the total energy. In order to evaluate the formation energy of such structures, we need to use much larger supercells than the primitive cell model. It is true that Okatov and Ivanovskii reported a few supercell calculations. However, results by the semiempirical calculations should be reexamined. They have not evaluated the formation energy, either.

Supercells of β-sialons composed of 56 atoms have been chosen so as to increase the number of Al-O bonds. The supercells are two-times larger along a and b axis than the primitive-cell models. The number of **k**-points used for the numerical integration was 12 in the whole Brillouin zone of the supercell. Total energy convergence with respect to both the supercell size and **k**-points sampling was checked better than 1 meV/(Al+O). Many kinds of atomic arrangements in the extended model were surveyed using $N_{\text{Al-O}}$ as an indicator. First-principles calculations were made only for selected candidates. Two of them will be explained. In the model of Fig. 10(a), Al and O atoms are arranged on $(1\bar{1}00)$ plane. It corresponds to $z=2$ and $N_{\text{Al-O}}=5.25$ per $Si_{6-z}Al_zO_zN_{8-z}$. In the model of Fig. 10(b), Al and O atoms form a column along the c axis. The ordered structure is similar to the ''quasi-1D channel'' structure proposed by Okatov and Ivanovskii.[18] It corresponds to $z=1.5$ and $N_{\text{Al-O}}=6$, which shows maximum $N_{\text{Al-O}}$ at the composition according to Eq. (1).

The formation energies by the two models are 0.15 and 0.09 eV/Al+O, respectively. Although they are slightly smaller than the lowest formation energies by the primitive cell models with $z=1$ or 2, they are greater than the value at the segregation limit. These results seemingly suggest eventual phase separation of β-sialons, which contradicts to the experimental facts that sialons keep their original crystal structure up to a certain z value. They do not show phase separation by any diffraction techniques. A probable reason for the inconsistency can be due to the complete neglect of entropy terms in the present discussion. Both configurational and vibrational entropy terms should be taken into account when one discusses thermodynamical stability of compounds. Inclusion of the entropy terms may decrease the free energy of formation to stabilize the sialon phases at elevated temperatures where the sialons are normally synthesized. If this is the case, both β and spinel sialons may have a tendency to show phase separation at low temperatures where the entropy terms are small. This type of experiment may, however, be practically difficult because of low atomic diffusivity at low temperatures. The formation of local structures as shown in Figs. 10(a) and 10(b) has smaller energy benefit than the phase separation. Ordering of solute atoms to form a unique local structure as proposed in literatures may therefore be not likely to take place. Instead of forming such a unique structure, various kinds of Al+O rich domains may be coexistent in real β-sialon materials.

Finally let us provide a few words on the dependence of bond-lengths and band-gaps on the cell size. The optimized structure showing the lowest formation energy among the present supercell calculations was that of Fig. 10(b). It shows $E_g=4.1$ eV, $d_{\text{Al-O}}=1.75$, $d_{\text{Al-N}}=1.75$, $d_{\text{Si-N}}=1.72$, and $d_{\text{all}}=1.73$ Å, which are not significantly different from those shown in Figs. 4 and 8 by the primitive cell models. Theoretical atomic and electronic structures by the primitive cell models should therefore be quantitatively useful.

IV. CONCLUSION

We have studied atomic and electronic structures of β- and spinel-sialons ($Si_{6-z}Al_zO_zN_{8-z}$) in detail by means of *ab initio* plain-wave pseudopotential calculations. Results can be summarized as follows.

(1) Arrangements of solute atoms are systematically investigated using the primitive cell models of β- and spinel-sialons. Al-O and Si-N bonds are significantly preferred than Al-N and Si-O bonds in both of the solid solutions. They satisfactorily agree with experimental results by NMR in literature.

(2) Electronic structures of the lowest energy models exhibit few impuritylike states near the band edges. The band gap can be roughly approximated as the weighed average of those for end members, i.e., Si_3N_4 and Al_3O_3N. This is consistent to visible transparency of all β-sialons by experiments. Much smaller band gaps as predicted in an early theoretical work can be ascribed to the absence of structural optimization.

(3) Average bond-lengths of Al-X and Si-X (X=O,N) in the optimized structures are almost constant and independent of z. Magnitude of the atomic relaxation is found to be very small in the lowest energy models that are enriched by Al-O and Si-N bonds. These results show good agreements with the information obtained by EXAFS experiments.

(4) Calculations of formation energies of β-sialons using supercells composed of 56 atoms suggest that ordering of solute atoms to form a unique local structure is not likely to take place.

ACKNOWLEDGMENTS

This work was supported by the grant-in-aid for priority area (No. 751) from MEXT of Japan.

*Author to whom all correspondences should be addressed. Email address: kazu@cms.MTL.kyoto-u.ac.jp

†Present address: Japan Fine Ceramics Center, Atsuta, Nagoya, 456-8587 Japan.

[1] A. Zerr, G. Miehe, G. Serghiou, M. Schwarz, E. Kroke, R. Riedel, H. Fueß, P. Kroll, and R. Boehler, Nature (London) **400**, 340 (1999).

[2] S.-D. Mo, L. Ouyang, W. Y. Ching, I. Tanaka, Y. Koyama, and R. Riedel, Phys. Rev. Lett. **83**, 5046 (1999).

[3] F. Oba, K. Tatsumi, H. Adachi, and I. Tanaka, Appl. Phys. Lett. **78**, 1577 (2001).

[4] Y. Oyama and O. Kamigaito, Jpn. J. Appl. Phys. **10**, 1637 (1971).

[5] K. H. Jack and W. I. Wilson, Nature (London) **238**, 28 (1972).

[6] T. Sekine, H. He, T. Kobayashi, M. Tansho, and K. Kimoto, Chem. Phys. Lett. **344**, 395 (2001).

[7] F. K. Van Dijen, R. Metselaar, and R. B. Helmholdt, J. Mater. Sci. Lett. **6**, 1101 (1987).

[8] C.-K. Loong, J. W. Richardson, Jr., S. Sukuzi, and M. Ozawa, J. Am. Ceram. Soc. **79**, 3250 (1996).

[9] N. D. Butler, R. Dupree, and M. H. Lewis, J. Mater. Sci. Lett. **3**, 469 (1984).

[10] R. Dupree, M. H. Lewis, G. Leng-Ward, and D. S. Williams, J. Mater. Sci. Lett. **4**, 393 (1985).

[11] R. Dupree, M. H. Lewis, and M. E. Smith, J. Appl. Crystallogr. **21**, 109 (1988).

[12] M. E. Smith, J. Phys. Chem. **96**, 1444 (1992).

[13] J. Sjöberg, T. Ericsoon, and O. Lindqvist, J. Mater. Sci. **27**, 5911 (1992).

[14] I. Tanaka, S. Nasu, H. Adachi, Y. Miyamoto, and K. Niihara, Acta Metall. Mater. **40**, 1995 (1992).

[15] W-Y. Ching, M-Z. Huang, and S-D. Mo, J. Am. Ceram. Soc. **83**, 780 (2000).

[16] I. Tanaka, G. Pezzotti, T. Okamoto, Y. Miyamoto, and M. Koizumi, J. Am. Ceram. Soc. **72**, 1656 (1989).

[17] Y. Fujiwara, I. Tanaka, T. Okamoto, S. Kume, and Y. Miyamoto, J. Ceram. Soc. Jpn. **98**, 360 (1990).

[18] S. V. Okatov and A. L. Ivanovskii, Int. J. Inorg. Mater. **3**, 923 (2001).

[19] V. Milman, B. Winkler, J. A. White, C. J. Pickard, M. C. Payne, E. V. Akhmatskaya, and R. H. Nobes, Int. J. Quantum Chem. **77**, 895 (2000).

[20] J. P. Perdew, J. A. Chevary, S. H. Vosko, K. A. Jackson, M. R. Pederson, D. J. Singh, and C. Fiolhais, Phys. Rev. B **46**, 6671 (1992).

[21] D. Vanderbilt, Phys. Rev. B **41**, 7892 (1990).

[22] H. J. Monkhorst and J. D. Pack, Phys. Rev. B **13**, 5188 (1976).